Hindawi
Mathematical Problems in Engineering
Volume 2020, Article ID 6874870, 11 pages
https://doi.org/10.1155/2020/6874870

Research Article

The Hybrid Finite Difference and Moving Boundary Methods for Solving a Linear Damped Nonlinear Schrödinger Equation to Model Rogue Waves and Breathers in Plasma Physics

Alvaro H. Salas,[1,2] **S. A. El-Tantawy**,[3,4] **and Jairo E. Castillo H.**[5]

[1]*Department of Mathematics, Universidad Nacional de Colombia, Sede Bogotá 111321, Bogotá, Colombia*
[2]*Universidad Nacional de Colombia-Nubia Campus Department of Mathematics and Statistics FIZMAKO Research Group, Bogotá, Colombia*
[3]*Department of Physics, Faculty of Science, Port Said University, Port Said 42521, Egypt*
[4]*Research Center for Physics (RCP), Department of Physics, Faculty of Science and Arts, Al-Baha University, Al-Baha, Saudi Arabia*
[5]*Universidad Distrital Francisco José de Caldas, FIZMAKO Research Group, Bogotá, Colombia*

Correspondence should be addressed to Alvaro H. Salas; ahsalass@unal.edu.co and S. A. El-Tantawy; samireltantawy@yahoo.com

Received 28 May 2020; Accepted 5 August 2020; Published 1 October 2020

Academic Editor: Luigi Rodino

In this paper, the dissipative and nondissipative modulated pulses such as rogue waves (RWs) and breathers (Kuznetsov-Ma breathers and Akhmediev breathers) that can exist and propagate in several fields of sciences, for example, plasma physics, have been analyzed numerically. For this purpose, the fluid dusty plasma equations with taking the kinematic dust viscosity into account are reduced to the linear damped nonlinear Schrödinger equation using a reductive perturbation technique. It is known that this equation is not integrable and, accordingly, does not have analytical solution. Thus, for modelling both dissipative RWs and breathers, the improved finite difference method is introduced for this purpose. It is found that FDM is a good numerical technique for small time interval but for large time interval it becomes sometimes unacceptable. Therefore, to describe these waves accurately, the new improved numerical method is considered, which is called the hybrid finite difference method and moving boundary method (FDM-MBM). This last and updated method gives an accurate and excellent description to many physical results, as it was applied to the dust plasma results and the results were good.

1. Introduction

A nonlinear Schrödinger-type equation [1], especially the cubic nonlinear Schrödinger equation (CNLSE) $(i\partial_t\psi + P\partial_x^2\psi + Q|\psi|^2\psi = 0)$, is one of the most universal models that describe many physical nonlinear systems. Here, $\psi \equiv \psi(x,t)$ represents a complex function, and the two coefficients P and Q represent the coefficients of the dispersion and nonlinear terms, respectively. It is understood that the values P and Q are functions in relevant physical configurational parameters such as temperature, pressure, particles density, entropy, and many other physical parameters according to the physical model in question. The CNLSE and many others (partial and ordinary) differential equations were used to interpret many mysterious phenomena that occur in various fields of sciences [2–17]. The CNLSE can support various exact analytic solutions; some of them depend on a zero background such as modulated envelope bright-, dark-, and gray-solitons [8, 9]. Several monographs and numerous published papers have been devoted to analyze the CNLSE, which possess special solution in the form of dark solitons which retain their velocities and shapes after interaction amongst themselves [18–20]. On the other side, some of these solutions are based on a finite background such as the breather structures (which include periodic space and localized time Akhmediev breathers (ABs) in addition to periodic time and localized space Kuznetsov-Ma (KM) soliton) and rogue waves (RWs) [10–17]. Rogue waves (RWs), freak waves (FWs), huge

waves, killer waves, and so forth (all names are synonymous) are known to be an unstable phenomenon that generally exists in nonlinear and dispersive systems [21]. RWs are characterized by several properties that differ from the surrounding waves, which can be generated and found at the same time in the physical system. One of the most important characteristics is that the RWs are localized in space-time [12]. Also, their amplitude may be equal to three times of the adjacent/carrier amplitudes (we mean here the first-order RWs but the super RWs have amplitudes higher than 3 times the surrounding waves [13, 22–24]). Physically, these types of huge waves suck high energy from the surrounding pulses, which amplifies their amplitude. Moreover, the RWs are instantaneous pulses, where they appear suddenly and suddenly disappear without a trace [25]. These waves (first-order and second-order RWs) have been observed and generated in laboratory in various fields, including water tank [13–15], electronegative plasmas [26–28], optics [29–31], Bose-Einstein condensates (BEC) [32], superfluid helium [33], capillary phenomena [34], and microwaves [35]. Also, Optical RWs in telecommunication data streams are investigated theoretically [36] and observed in the atmosphere [37].

The CNLSE is a good mathematical model for explaining a huge number of mysterious phenomena that appear in nature, mechanical systems, superfluidity in the absence of frictional forces such as viscosity, collision between charged and neutral particles, and so forth. However, if the effect of collisional frequencies between the charged and neutral particles and the effect of the particles viscosity are taken into account, the standard CNLSE becomes not suitable to investigate the impact of these forces on the nonlinear phenomena that can propagate in the physical medium. Accordingly, the linear damped CNLSE (dCNLSE) ($i\partial_t\psi + P\partial_x^2\psi + Q|\psi|^2\psi + iR\psi = 0$) [38–47] was used in place of the standard CNLSE for studying the impact of fractional forces on the modulational instability (MI) of the modulated structures and associated damping waves. Here, R refers to the coefficient of the linear damping term and both CNLSE and dCNLSE can be derived from the fluid plasma equations using a reductive perturbation method (RPM) (the derivative expansion method (DEM)) [22–25, 41–46]. The dCNLSE was derived for several plasma systems using the derivative expansion method in order to study its modulational instability (MI) of dissipative modulated structures including the dissipative/damping breathers and RWs in a collisional plasma [41–46]. Most of the previous studies focused on transforming the nonintegrable dCNLSE into the integrable CNLSE using an appropriate transformation [40] in order to investigate envelope solitons, breathers, RWs, cnoidal waves, and so forth. Recently, El-Tantawy et al. [46] studied the dissipative RWs and ABs in electron depleted complex plasmas by analyzing the dCNLSE using Wolfram Mathematica package version 11.3 and without using any transformation. In the present study, we will restrict our attention to solving and analyzing both CNLSE and dCNLSE numerically using the improved finite difference method (FDM) with the moving boundary method (MBM). To do that, an exact analytic solution to the CNLSE will be used as initial solution to find the numerical approximate solutions to both CNLSE and dCNLSE. Also, we will discuss a series of various solutions that are supported by the CNLSE.

2. Physical Problem and Mathematical Model

A depleted electron complex plasma consisting of inertia negative dust grains and inertialess two non-Maxwellian positive ions with different two temperatures is considered. In this model, the restoring force comes from the pressures of two positive ions, while the mass of the negative dust particles is responsible for the inertia. Moreover, it is assumed that the density of the electrons has been sufficiently depleted due to the charge of dust grains which this process has observed in the laboratory [48] and in space in many situations [49]. It is assumed that $Z_d n_d^{(0)} \gg n_e^{(0)}$ and the mass of the dust grains are the same, where $n_e^{(0)}$ donates the electron unperturbed density. Thus, the quasi-neutrality condition can be written as $Z_d n_d^{(0)} = n_h^{(0)} + n_c^{(0)}$ which leads to $1 = \mu_c + \mu_h$, where $n_j^{(0)}$ represents the unperturbed number density of the j^{th} species (here, $j = d$, h, and c, for the negative dust impurities, the hot positive ion, and cold positive ion, respectively), $\mu_c = n_c^{(0)}/(Z_d n_d^{(0)})$ gives the concentration of cold positive ion, $\mu_h = n_h^{(0)}/(Z_d n_d^{(0)})$ refers to the concentration of hot positive ion, and Z_d expresses the number of electrons residing on the surface of the dust particles [46]. It is clear that the electron number density $n_e^{(0)}$ is not included in the quasi-neutrality condition, which means that the electrons are completely depleted during the process of charging dust grains [50]. Thus, the normalized fluid basic equations that are governed in the nonlinear dynamics of dust-acoustic waves (DAWs) are given by the following continuity and momentum equations of the dust grains, respectively [46, 51–53]:

$$\partial_t n_d + \partial_x\left(n_d u_d\right) = 0, \tag{1}$$

$$\partial_t u_d + u_d\partial_x u_d = \partial_x\phi + \eta\partial_{x,x}^2 u_d, \tag{2}$$

where n_d and u_d represent the normalized number density and fluid velocity of dust grains, respectively, ϕ is the normalized electrostatic wave potential, η is the normalized dust kinematic viscosity, and x and t denote the normalized space and time variables, respectively. More details about this plasma model and the normalized technique can be found in [46, 51–53].

The non-Maxwellian normalized densities of cold and hot positive ions can be modelled by the following superthermal distribution [51, 52].

$$n_s = \mu_s\left[1 + \frac{\theta_s\phi}{\left(\kappa_s - (3/2)\right)}\right]^{-\kappa_s+(1/2)}, \tag{3}$$

where $s = c$ and h for the cold and hot positive ions, respectively; and $\theta_h \equiv \theta = T_c/T_h$ and $\theta_c = 1$ where T_s and $\kappa_s\,(>3/2)$ indicate the temperature and the spectral index of $s-$species, respectively.

The above system of equations (1)–(3) are closed by the following normalized Poisson's equation:

$$\partial_{x,x}^2\phi = n_d - (n_c + n_h) = 0. \tag{4}$$

The derivative expansion method (DEM) was devoted to reduce the governing equations (1)–(4) to the following dCNLSE:

$$i\partial_t\psi + \frac{1}{2}P\partial_x^2\psi + Q|\psi|^2\psi + iR\psi = 0. \tag{5}$$

Here, $\psi \equiv \psi(x,t)$ represents a complex function and the details of deriving equation (5) and the values of the coefficients P, Q, and R exist in [46]. It is understood that values of the coefficients P, Q, and R are functions of relevant plasma parameters.

It is known that the theory of MI is one of the most important effective mechanisms that have succeeded in explaining the propagation of modulated structures such as breathers, RWs, and envelope solitons in nonlinear mediums [22–25, 54–56]. The CNLSE ($R = 0$) is considered as one of the simplest global models that are used to study the MI of quasi-monochromatic modulated structures in weak dispersive-nonlinear medium such as different plasma models [22–25, 54–56]. After applying the linear theory of MI [22–25, 57, 58], it was proven that the product PQ is a necessary and sufficient condition for determining the (un) stable regions in which different types of modulated envelope structures can propagate in the physical model such as plasma physics and optical fiber. Accordingly, for $PQ < 0$, the modulated structures become stable and the dark envelope solitons can exist and propagate in the physical model. On the contrary, for $PQ > 0$, the modulated structures become unstable and in this case the bright envelope solitons and breathers structures in addition to Peregrine soliton (first-order RWs) can exist and generate in the physical model [22–25, 57, 58]. If the damping term is taken into account, that is, $R \neq 0$, the product PQ is not sufficient to determine the (un)stable regions of the modulated structures, and this requires an additional condition in order to restrict these regions precisely. We will mention these conditions and explain them briefly because they exist in detail in many published papers [41, 42, 45, 46, 59]. For studying the MI of equation (5), the theory of linear instability is introduced and, after applying this theory, it was found that the damped modulated structures become unstable if $PQ > 0 \& t < t_{\max}$, where $t_{\max} = (1/2R)\ln[2Q|\psi_0|^2/(PK^2)]$ gives the period of the MI, $K (\ll k)$ represents the wavenumber of modulated structures, k expresses the carrier wavenumber, and ψ_0 indicates the amplitude of the pumping carrier wave [46]. It should be noted that if the propagation time becomes larger than the period of the MI, that is, $\tau > \tau_{\max}$, even if $PQ > 0$, then the modulated structures become stable (more details can be found in [46]).

3. Methods of Solution

3.1. The Algorithm of FDM. Let us define the following initial value problem (IVP):

$$i\partial_t\psi + \frac{1}{2}P\partial_x^2\psi + Q|\psi|^2\psi + iR\psi = 0, \tag{6}$$

which is subjected to the initial condition

$$\psi(x, T_i) = \varphi(x), \tag{7}$$

where $\Omega = [L_i, L_f] \times [T_i, T_f]$ represents the space-time domain and $\varphi(x)$ represents the exact analytic solution to the undamped CNLSE, that is, equation (6) for $R = 0$.

In order to solve the IVP in (6) and (7), the improved finite difference method (FDM) is devoted for this purpose. To do that, let us firstly divide the complex wave function $\psi(x,t) \equiv \psi$ into two parts, real and imaginary parts, as follows:

$$\psi = V + iW, \tag{8}$$

and, by inserting equation (8) into equation (6) and separating both the real and the imaginary parts, the following coupled system of partial differential equations (PDEs) is obtained:

$$\left.\begin{aligned} &\frac{1}{2}\left(PV\partial_x^2V - W\left(P\partial_x^2W + 2R\right) - 2\partial_tW\right) + QV\left(V^2 + W^2\right) = 0,\\ &\frac{1}{2}P\partial_x^2VW + V\left(\frac{1}{2}P\partial_x^2W + R\right) + QW\left(V^2 + W(x,t)^2\right) + \partial_tV = 0, \end{aligned}\right\} \tag{9}$$

where $V \equiv V(x,t)$ and $W \equiv W(x,t)$.

For solving equation (5) in the domain Ω, let us divide this domain into the following uniform mesh sizes:

$$\begin{aligned} \Delta x &= \frac{L_f - L_i}{m},\\ x_k &= L_i + \frac{L_f - L_i}{\Delta x}k,\\ \Delta t &= \frac{T_f - T_i}{n},\\ t_j &= T_i + \frac{T_f - T_i}{\Delta t}j, \end{aligned} \tag{10}$$

where m and n denote two positive integer numbers, $k = 0, 1, 2, \ldots, m$ and $j = 0, 1, 2, \ldots, n$.

The finite difference formulas are introduced to estimate the first derivative of time $\partial_t(\cdot)$ and the second derivative of space $\partial_x^2(\cdot)$ as follows:

$$\partial_tV\left(x_k, t_j\right) \approx \frac{V_{k,j+1} - V_{k,j}}{\Delta t}, \tag{11}$$

for $j = 0, 1, 2, 3$,

$$\partial_tV\left(x_k, t_j\right) \approx \left(\frac{1}{840\Delta t}\right)\left(\begin{array}{l} 3V_{i,j-4} - 32V_{i,j-3} + 168V_{i,j-2} - 672V_{i,j-1}\\ +672V_{i,j+1} - 168V_{i,j+2} + 32V_{i,j+3} - 3V_{i,j+4} \end{array}\right), \tag{12}$$

for $4 \leq j \leq n-4$ $(n \geq 8)$, and

$$\partial_t V\left(x_k, t_j\right) \approx \frac{V_{k,j} - V_{k,j_{-1}}}{\Delta t}, \tag{13}$$

for $j = n-3, n-2, n-1, n$.

For the second derivative of space $\partial_x^2(\cdot)$, the following formulas are defined:

$$\partial_x^2 V\left(x_k, t_j\right) \approx \frac{V_{k,j} - 2V_{k+1,j} + V_{k+2,j}}{\Delta x^2}, \tag{14}$$

for $k = 0, 1, 2, 3$,

$$\partial_x^2 V\left(x_k, t_j\right) \approx -\frac{V_{k-2,j} - 16V_{k-1,j} + 30V_{k,j} - 16V_{k+1,j} + V_{k+2,j}}{12\Delta x^2}, \tag{15}$$

for $2 \le k \le m-2$ $(m \ge 4)$, and

$$\partial_x^2 V\left(x_k, t_j\right) \approx \frac{V_{k-2,j} - 2V_{k-1,j} + V_{k,j}}{\Delta x^2}, \tag{16}$$

for $k = m-2, m-1, m$.

$\partial_t W(x_k, t_j)$ and $\partial_x^2 W(x_k, t_j)$ have similar formulas.

The system of equation (9) can be written in the following discretization form:

$$\left.\begin{aligned} &\frac{1}{2}\left(PV_{k,j}\partial_x^2 V\left(x_k, t_j\right) - W_{k,j}\left(P\partial_x^2 W\left(x_k, t_j\right) + 2R\right) - 2\partial_t W\left(x_k, t_j\right)\right) + QV_{k,j}\left(V_{k,j}^2 + W_{k,j}^2\right) = 0, \\ &\frac{1}{2}P\partial_x^2 W\left(x_k, t_j\right)W_{k,j} + V_{k,j}\left(\frac{1}{2}P\partial_x^2 W\left(x_k, t_j\right) + R\right) + QW_{k,j}\left(V_{k,j}^2 + W_{k,j}^2\right) + \partial_t V\left(x_k, t_j\right) = 0. \end{aligned}\right\} \tag{17}$$

The following boundary conditions will be considered during our analysis:

$$\left.\begin{aligned} v_{k,0} &= \Re\left[\varphi\left(x_k, 0\right)\right], \\ w_{k,0} &= \Im\left[\varphi\left(x_k, 0\right)\right], \end{aligned}\right\} \tag{18}$$

where $k = 0, 1, 2, \ldots, m$.

System (17) is not linear and we may solve it by means of the Newton-Raphson method. Let us consider some examples concerning both undamped and damped cases. This method works well for small time intervals. This corresponds to the practical values of the period of the existence and propagation of the acoustic modulated structures within the plasma medium. However, for large time intervals, we may apply the hybrid method: FDM with moving the boundary method (MBM) by small amounts of time as described in the following section.

3.2. The Algorithm of MBM. Suppose that we already solved the IVP in (6) and (7) in the intervals $L_i \le x \le L_f$ and $T_i \le x \le T_i + \mathrm{d}\tau$ and let $\psi_0(x,t)$ be the approximate solution to the IVP in (6) and (7). So, we define

$$\varphi_0(x) = \psi_0\left(x, T_1 + \mathrm{d}\tau\right), \tag{19}$$

where $\mathrm{d}\tau$ refers to small positive number in the interval $[T_i, T_f]$.

After that, we move the boundary by small amount of time that equals $\mathrm{d}\tau$. Then, the IVP in (6) and (7) can be rewritten in the following form:

$$i\partial_t\psi + \frac{1}{2}P\partial_x^2\psi + Q|\psi|^2\psi + iR\psi = 0, \tag{20}$$

$$\left.\begin{aligned} &L_i < x < L_f, \\ &T_i + \mathrm{d}\tau < t < T_i + 2\mathrm{d}\tau, \end{aligned}\right\} \tag{21}$$

and its solution in the time interval $T_i + \mathrm{d}\tau < t < T_i + 2\mathrm{d}\tau$ reads

$$\psi\left(x, T_1 + \mathrm{d}\tau\right) = \varphi_0(x). \tag{22}$$

We will continue to repeat this step until reaching the final time T_f at $T_i + m\mathrm{d}\tau$, where $m = \lfloor (T_2 - T_1)/\mathrm{d}\tau \rfloor$. Thereafter, we can get

$$\psi(x,t) = \psi_r(x,t), \tag{23}$$

for $T_i + r\mathrm{d}\tau \le t \le T_i + (r+1)\mathrm{d}\tau$ and $r = 0, 1, 2, \ldots, m = [(T_f - T_i)/\mathrm{d}\tau]$.

Observe that $\psi_r(x,t)$ is an approximate initial solution to the IVP:

$$\left.\begin{aligned} &i\partial_t\psi + \frac{1}{2}P\partial_x^2\psi + Q|\psi|^2\psi + iR\psi = 0, \\ &L_1 < x < L_2, \\ &T_1 + r\mathrm{d}\tau \le t \le T_1 + (r+1)\mathrm{d}\tau, \end{aligned}\right\} \tag{24}$$

$$\psi\left(x, T_1 + r\mathrm{d}\tau\right) = \varphi_{r-1}(x) = \psi_{r-1}\left(x, T_1 + r\mathrm{d}\tau\right).$$

4. FDM-MBM for Analyzing RWs and Breathers

Let us consider and introduce some illustrative and useful examples. In the following sections, the above hybrid FDM-MBM will be applied on both undamped CNLSE and damped CNLSE for analyzing some dissipative and nondissipative modulated structures (RWs and breathers) that can propagate in many nonlinear mediums such as optical fiber and plasma physics.

In absence of linear damping term $(R = 0)$ and in the unstable regions $(PQ > 0)$, the nonintegrable dCNLSE (6) is reduced to the integrable CNLSE:

$$i\partial_t\psi + \frac{1}{2}P\partial_x^2\psi + Q|\psi|^2\psi = 0, \tag{25}$$

This equation is completely integrable and supports many exact analytical solutions as we mentioned earlier, such as envelope solitons, RWs, and breathers. Thus, the exact RWs and breathers solution to equation (25) in the compact form reads [31, 60]

$$\psi = \sqrt{\frac{P}{Q}}\left[1 + \frac{2(1-2\delta)\cosh[h_1 Pt] + ih_1\sinh[h_1 Pt]}{\sqrt{2\delta}\,\cos(h_2 x) - \cosh[h_1 Pt]}\right]\exp(iPt), \tag{26}$$

and, here, $\sqrt{P/Q}$ indicates the background amplitude, and the parameter δ is called the transfer switch which is responsible for determining the type of waves through controlling the value of the following relationships: $h_1 = \sqrt{8\delta(1-2\delta)}$ and $h_2 = \sqrt{4(1-2\delta)}$. Thus, solution (26) can describe three types of solutions as follows: (i) for $\delta < 0.5$, the localized time and periodic-space structure can be obtained, which is called Akhmediev breathers (ABs) solution; (ii) for $\delta > 0.5$, the localized space and time-periodic structures are covered, which are called Kuznetsov-Ma (KM) breathers solution; and, finally, (iii) for $\lim\delta \longrightarrow 0.5$, the localized time-space structures are covered, which are called first-order rogue wave (RW)/Peregrine soliton/Peregrine breathers solution.

4.1. Numerical Simulations to (Non)dissipative RWs and Breathers. For Peregrine soliton (first-order RW) solution, solution (??) can be reduced to the following traditional form of RWs:

$$\begin{aligned}\psi_{\mathrm{RWs}} &= \lim_{\delta\longrightarrow 0.5}(\psi) = \sqrt{\frac{P}{Q}}\left[-1 + \frac{4}{G}(1+2iPt)\right]\exp(iPt)\\ &\equiv \sqrt{\frac{P}{Q}}\left[1 - \frac{4}{G}(1+2iPt)\right]\exp(iPt)\\ &\equiv V_{\mathrm{RWs}} + iW_{\mathrm{RWs}},\end{aligned} \tag{27}$$

with

$$\begin{aligned}V_{\mathrm{RWs}} &= \left(\frac{1}{G}\right)\sqrt{\frac{P}{Q}}[(G-4)\cos(Pt) + 8Pt\sin(Pt)],\\ W_{\mathrm{RWs}} &= \left(\frac{1}{G}\right)\sqrt{\frac{P}{Q}}[(G-4)\sin(Pt) - 8Pt\cos(Pt)],\end{aligned} \tag{28}$$

where $G = (1 + 4x^2 + 4P^2t^2)$. To apply the hybrid FDM-MBM for analyzing the (non)dissipative RWs, the following initial condition is introduced:

$$\begin{aligned}\psi_{\mathrm{RWs}}(x, T=0) &= \psi_{\mathrm{RWs}}(x)\\ &\equiv \sqrt{\frac{P}{Q}}\,\frac{\left(4x^2-3\right)}{\left(4x^2+1\right)},\end{aligned} \tag{29}$$

where $x \in [L_i, L_f]$ and $T \in [T_i, T_f]$.

For the Kuznetsov-Ma (KM) breathers solution ($\delta > 1/2$), the exact analytic solution can be written in the following form:

$$\psi_{\mathrm{KM}} = V_{\mathrm{KM}} + iW_{\mathrm{KM}}, \tag{30}$$

with

$$\begin{aligned}V_{\mathrm{KM}} &= \sqrt{\frac{P}{Q}}\,\frac{[(4\delta-1)\cos(g_1 Pt) - \sqrt{2\delta}\cosh(g_2 x)]}{[\cos(g_1 Pt) - \sqrt{2\delta}\cosh(g_2 x)]},\\ W_{\mathrm{KM}} &= \sqrt{\frac{P}{Q}}\,\frac{g_1\sin(g_1 Pt)}{[\cos(g_1 Pt) - \sqrt{2}\,\sqrt{\delta}\,\cos(g_2 x)]},\end{aligned} \tag{31}$$

and the following initial condition will be used in the hybrid FDM-MBM to analyze (non)dissipative KM breathers numerically:

$$\begin{aligned}\psi_{\mathrm{KM}}(x, T=0) &= \psi_{\mathrm{KM}}(x)\\ &\equiv \sqrt{\frac{P}{Q}}\left[\frac{2(1-2\delta)}{\sqrt{2}\,\sqrt{\delta}\cosh(g_2 x) - 1} + 1\right],\end{aligned} \tag{32}$$

where $g_1 = \sqrt{8\delta(2\delta-1)}$ and $g_2 = \sqrt{4(2\delta-1)}$.

For the ABs solution ($\delta < 1/2$), the following form of the exact analytic solution is considered:

$$\psi_{\mathrm{ABs}} = V_{\mathrm{ABs}} + iW_{\mathrm{ABs}}, \tag{33}$$

with

$$\begin{aligned}V_{\mathrm{ABs}} &= \sqrt{\frac{P}{Q}}\,\frac{[(1-4\delta)\cosh(h_1 Pt) + \sqrt{2\delta}\,\cos(h_2 x)]}{[\sqrt{2\delta}\,\cos(h_2 x) - \cosh(h_1 Pt)]},\\ W_{\mathrm{ABs}} &= \sqrt{\frac{P}{Q}}\,\frac{h_1\sinh(h_1 Pt)}{\sqrt{2\delta}\cos(h_2 x) - \cosh(h_1 Pt)}.\end{aligned} \tag{34}$$

For analyzing (non)dissipative ABs numerically via the hybrid FDM-MBM, the following initial solution at $T = 0$ is considered:

$$\begin{aligned}\psi_{\mathrm{ABs}}(x, T=0) &= \psi_{\mathrm{AB}}(x)\\ &\equiv \sqrt{\frac{P}{Q}}\,\frac{[(1-4\delta) + \sqrt{2\delta}\,\cos(h_2 x)]}{[1 - \sqrt{2\delta}\,\cos(h_2 x)]}.\end{aligned} \tag{35}$$

The comparisons between the exact analytic solutions of nondissipative RWs (27), KM breathers (30), and ABs (33) and the numerical simulation solutions using FDM are introduced in Figures 1(a), 2(a), and 3(a), respectively, for $P = Q = 2$, $R = 0$, $\Delta x = 0.2$, and $\Delta t = 0.25$. Also, in Figures 1(b), 2(b), and 3(b) and for $P = Q = 2$, $R = 0.5$, $\Delta x = 0.2$, and $\Delta t = 0.25$, the numerical simulation solutions using FDM for dissipative RWs and dissipative breathers are compared to the following approximate analytical solutions (sometimes are called semianalytical solutions):

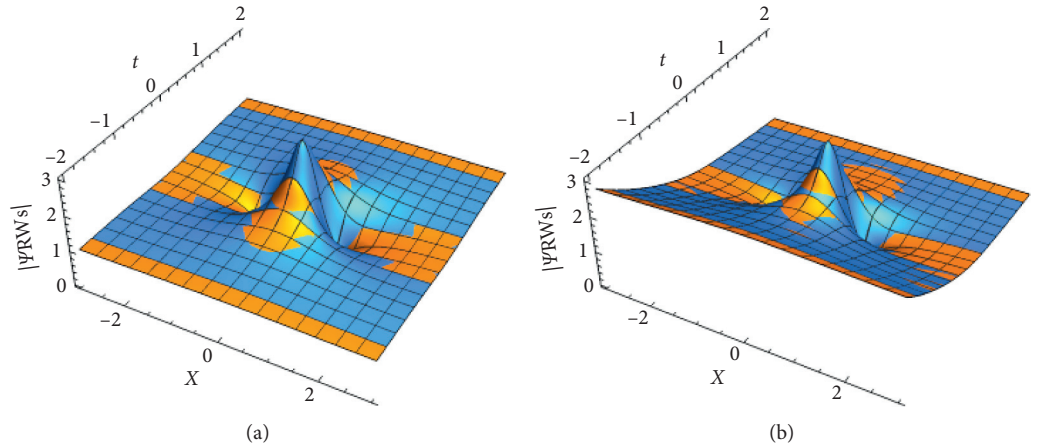

Figure 1: A comparison between the approximate numerical solution using FDM and (a) the exact solution to nondissipative RWs (27) and (b) the approximate analytical dissipative RWs solution (36).

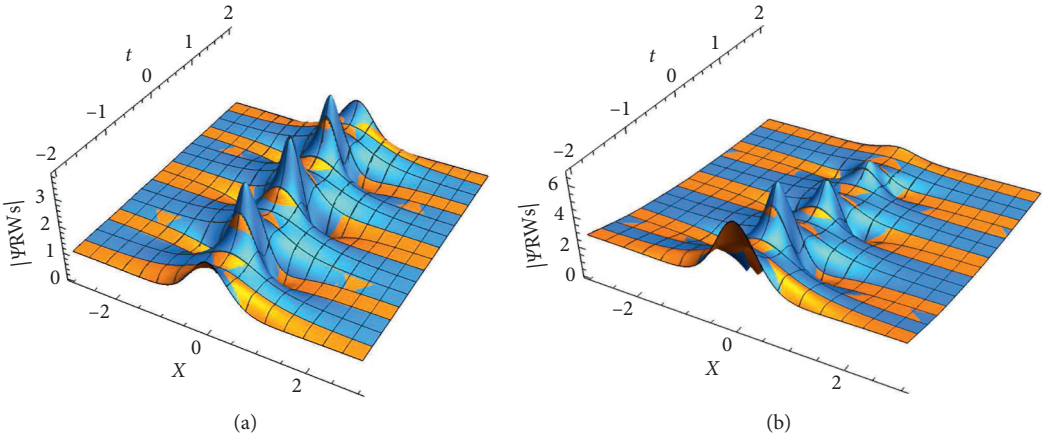

Figure 2: A comparison between the approximate numerical solution using FDM and (a) the exact solution to nondissipative KM breathers (30) and (b) the approximate analytical dissipative KM breathers solution (36).

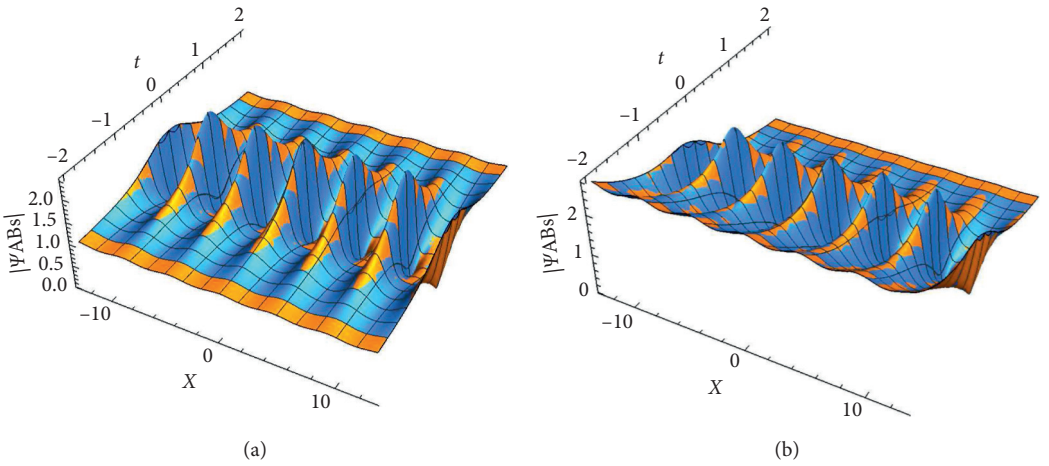

Figure 3: A comparison between the approximate numerical solution using FDM and (a) the exact solution to nondissipative ABs (33) and (b) the approximate analytical dissipative ABs solution (36).

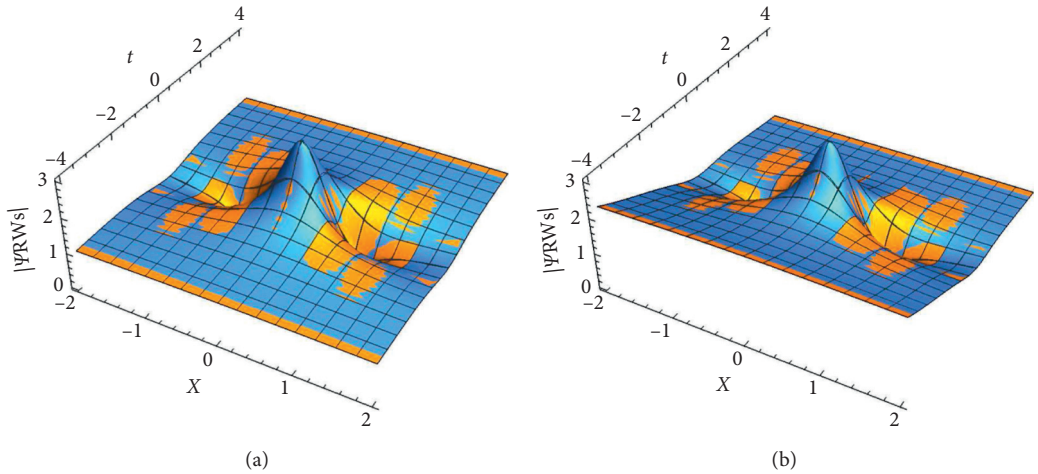

Figure 4: A comparison between the approximate numerical solution using FDM-MBM and (a) the exact solution to nondissipative RWs (27) and (b) the approximate analytical dissipative RWs solution (36).

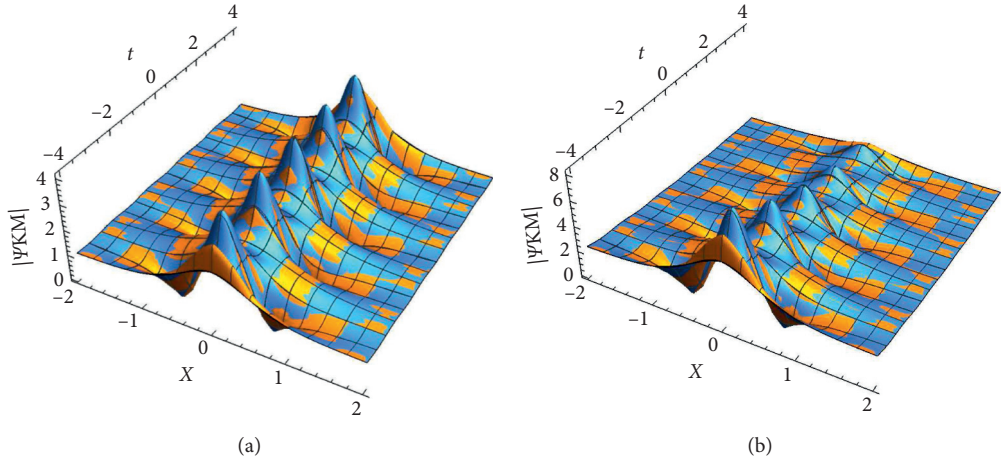

Figure 5: A comparison between the approximate numerical solution using FDM-MBM and (a) the exact solution to nondissipative KM breathers (30) and (b) the approximate analytical dissipative KM breathers solution (36).

$$\psi = (V + iW)\exp(-Rt), \tag{36}$$

with

$$(V, W) = \begin{matrix} V_{\mathrm{RWs}} & W_{\mathrm{RWs}} \\ V_{\mathrm{KM}} & W_{\mathrm{KM}} \\ V_{\mathrm{ABs}} & W_{\mathrm{ABs}} \end{matrix}\Bigg\}. \tag{37}$$

More details about the semianalytical solution (36) can be found in [61]. It is observed that the approximate numerical solutions using FDM for RWs and breathers give excellent results as compared to the exact analytic solutions and semianalytical solution (36) but in the small time interval and, for large time interval, the results become unacceptable, especially for KM breathers. Thus, the hybrid FDM-MBM is introduced to improve the numerical results, especially at large time interval. According to this method (hybrid FDM-MBM), the exact analytic solutions of nondissipative RWs (27), KM breathers (30), and ABs (33) are compared to the numerical simulation solutions as shown in Figures 4(a), 5(a), and 6(a), respectively, for $P = Q = 1$, $R = 0$, $\Delta x = 0.5$, $\Delta t = 0.01$, and $\Delta\tau = 0.25$. Furthermore, the comparisons between the semianalytical solutions (36) of dissipative RWs and dissipative breathers and the numerical simulation solutions using the hybrid FDM-MBM are presented in Figures 4(b), 5(b), and 6(b), respectively, for $P = Q = 1$, $R = 0.2$, $\Delta x = 0.5$, $\Delta t = 0.01$, and $\Delta\tau = 0.25$. Moreover, the effects of damping term on the RW and breathers profiles according to the physical plasma parameters $(k, \kappa_c, \kappa_h, \theta, \mu_c) = (3, 5.5, 3.5, 0.1, 0.2)$ are investigated in Figure 7. It is clear that the amplitudes of RWs and breathers decrease with increasing the viscosity coefficient which this behavior has observed in plasma experiments. The comparison results between the numerical simulation solutions and the semianalytical solutions showed the near-perfect compatibility between them. Finally, we can

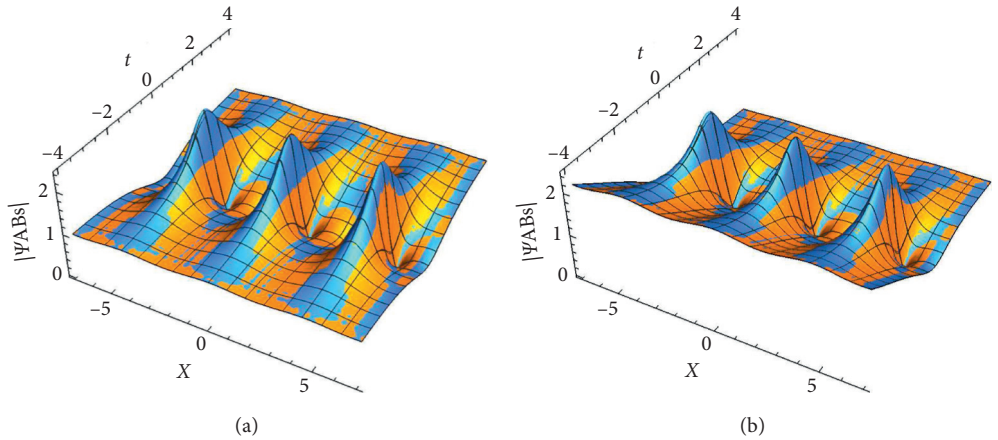

Figure 6: A comparison between the approximate numerical solution using FDM-MBM and (a) the exact solution to nondissipative ABs (33) and (b) the approximate analytical dissipative ABs solution (36).

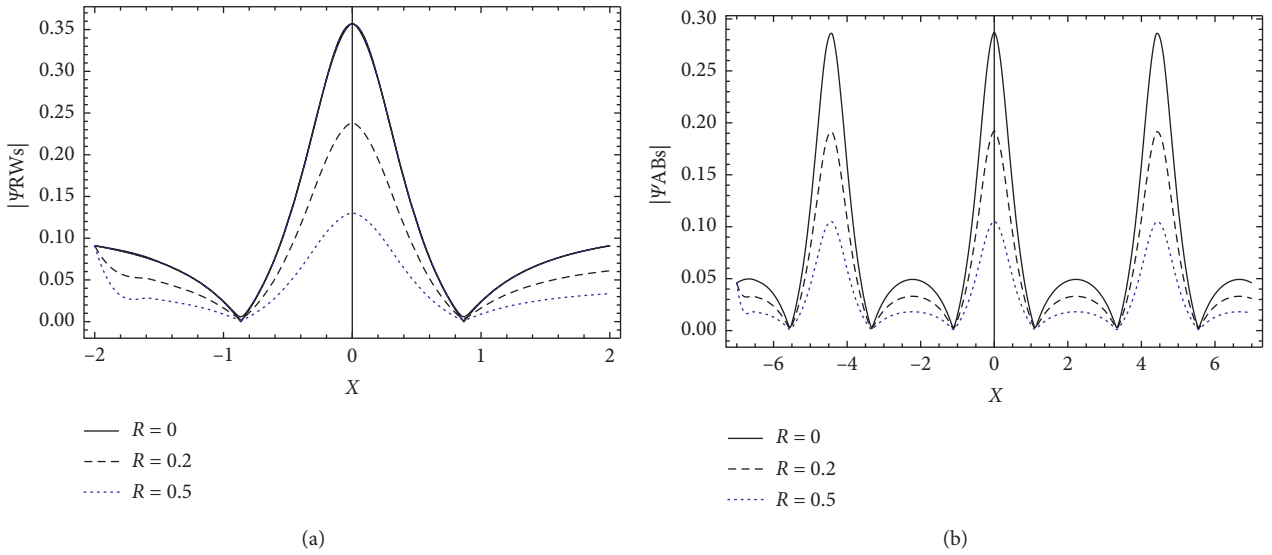

Figure 7: The profiles of dissipative (a) RWs and (b) ABs are plotted against x for different values of kinematic dust viscosity R.

conclude that the hybrid FDM-MBM gives strong and high accurate results with minimal time and effort. Also, this method does not need high computer capabilities to analyze data and all calculations can be done using a PC. But the FDM is faster than the hybrid FDM-MBM.

5. Conclusion

The propagation of both dissipative and nondissipative modulated nonlinear structures including freak waves and breathers (Kuznetsov-Ma breathers and Akhmediev breathers) in the nonlinear-dispersive media such as optical fiber and plasma physics has been investigated analytically and numerically in the framework of both cubic nonlinear Schrödinger equation (CNLSE) and linear damped cubic nonlinear Schrödinger equation (dCNLSE). As a physical application, the basic fluid equations for an electron depleted dusty plasma containing two different types on superthermal ions are reduced to the wave equation (dCNLSE) using the derivative expansion method. In the present plasma model, the kinematic dust viscosity is taken into account, which leads to the linear damping term appearing in the dCNLSE and if the dust viscosity is ignored, the standard CNLSE will be covered. The improved finite difference method (FDM) is devoted to solving both the CNLSE and dCNLSE for analyzing both dissipative and nondisssipative freak waves and breathers. It is found that the improved FDM gives excellent results for small time interval. This method is good in some physical applications such as the propagation of acoustic waves in different plasma models because the age of these waves is small compared to the age of the presence of plasma itself. However, for large time interval, the FDM gives reasonable results, but sometimes they are not so good. Consequently, the moving boundary method (MBM) is introduced besides the FDM to improve the obtained results at large time interval. In fact, it is noticed that the hybrid

method gives excellent results compared to the traditional method with many physical applications. For the future work, it is well known that most physical experiments that take place in the laboratory, especially experiments of plasma physics, are carried out in a cylindrical/spherical vessel [62–64]. Therefore, to describe the modulated envelope waves that can propagate in the cylindrical/spherical vessel, the basic equations of the physical problem must be designed in the curved coordinates/nonplanar (cylindrical and spherical) coordinates. Accordingly, we will obtain an elevation equation that can describe cylindrical and spherical modulated waves (dark solitons, bright solitons, freak waves, and breathers) in different physical environments, such as plasma physics. Thus, we will solve this problem using the hybrid method due to its good results.

Data Availability

No data were used to support this research.

Conflicts of Interest

The authors declare that they have no conflicts of interest.

References

[1] W. Gao, H. F. Ismael, A. M. Husien, H. Bulut, and H. M. Baskonus, "Optical soliton solutions of the cubic-quartic nonlinear Schrödinger and resonant nonlinear Schrödinger equation with the parabolic law," *Applied Sciences*, vol. 10, no. 1, pp. 219-220, 2020.

[2] P. K. Pandey, "A new computational algorithm for the solution of second order initial value problems in ordinary differential equations," *Applied Mathematics and Nonlinear Sciences*, vol. 3, no. 1, pp. 167–174, 2018.

[3] X.-J. Yang and F. Gao, "A new technology for solving diffusion and heat equations," *Thermal Science*, vol. 21, no. 1, pp. 133–140, 2017.

[4] X.-J. Yang, D. Baleanub, M. Lazarevic, and M. Cajic, "Fractal boundary value problems for integral and differential equations with local fractional operators," *Thermal Science*, vol. 19, no. 3, pp. 959–966, 2015.

[5] C. Cattani, "Biomedical signal processing and modeling complexity of living systems," *Computational Mathematical Methods in Medicine*, vol. 2012, Article ID 298634, 2 pages, 2012.

[6] C. Cattani, "Haar wavelet-based technique for sharp jumps classification," *Mathematical and Computer Modelling*, vol. 39, no. 2-3, pp. 255–278, 2004.

[7] M. Kolade, "Owolabi and ZakiaHammouch, spatiotemporal patterns in the Belousov–Zhabotinskii reaction systems with Atangana–Baleanu fractional order derivative," *Physica A*, vol. 523, pp. 1072–1090, 2019.

[8] A.-M. Wazwaz and S. A. El-Tantawy, "Optical Gaussons for nonlinear logarithmic Schrödinger equations via the variational iteration method," *Optik*, vol. 180, pp. 414–418, 2019.

[9] A. Biswas, "Chirp-free bright optical soliton perturbation with Fokas-Lenells equation by traveling wave hypothesis and semi-inverse variational principle," *Optik*, vol. 170, pp. 431–435, 2018.

[10] N. Akhmediev, J. M. Soto-Crespo, and A. Ankiewicz, "Extreme waves that appear from nowhere: on the nature of rogue waves," *Physics Letters A*, vol. 373, no. 25, pp. 2137–2145, 2009.

[11] Y.-C. Ma, "The perturbed plane-wave solutions of the cubic Schrödinger equation," *Studies in Applied Mathematics*, vol. 60, no. 1, pp. 43–58, 1979.

[12] D. H. Peregrine, "Water waves, nonlinear Schrödinger equations and their solutions," *The Journal of the Australian Mathematical Society. Series B. Applied Mathematics*, vol. 25, no. 1, pp. 16–43, 1983.

[13] A. Chabchoub, N. P. Hoffmann, and N. Akhmediev, "Rogue wave observation in a water wave tank," *Physical Review Letters*, vol. 106, no. 20, pp. 204502–204504, 2011.

[14] A. Chabchoub, N. Hoffmann, M. Onorato et al., "Observation of a hierarchy of up to fifth-order rogue waves in a water tank," *Physical Review E*, vol. 86, no. 5, pp. 56601–56606, 2012.

[15] A. Lechuga, "Rogue waves in a wave tank: experiments and modeling," *Natural Hazards and Earth System Sciences*, vol. 13, no. 11, pp. 2951–2955, 2013.

[16] O. G. Gaxiola and A. Biswas, "Akhmediev breathers, peregrine solitons and Kuznetsov-Ma solitons in optical fibers and PCF by Laplace-Adomian decomposition method," *Optik*, vol. 172, pp. 930–939, 2018.

[17] M. McKerr, I. Kourakis, and F. Haas, "Freak waves and electrostatic wavepacket modulation in a quantum electron–positron–ion plasma," *Plasma Physics and Controlled Fusion*, vol. 56, no. 3, pp. 35007–35017, 2014.

[18] S. A. El-Tantawy, W. M. Moslem, and R. Schlickeiser, "Ion-acoustic dark solitons collision in an ultracold neutral plasma," *Physica Scripta*, vol. 90, no. 8, p. 85606, 2015.

[19] S. A. El-Tantawy, A. M. Wazwaz, and R. Schlickeiser, "Solitons collision and freak waves in a plasma with Cairns-Tsallis particle distributions," *Plasma Physics and Controlled Fusion*, vol. 57, no. 12, p. 125012, 2015.

[20] S. A. El-Tantawy and A. M. Wazwaz, "Anatomy of modified Korteweg–de Vries equation for studying the modulated envelope structures in non-Maxwellian dusty plasmas: freak waves and dark soliton collisions," *Physics of Plasmas*, vol. 25, no. 9, p. 92105, 2018.

[21] Y.-Y. Tsai, J.-Y. Tsai, and I. Lin, "Generation of acoustic rogue waves in dusty plasmas through three-dimensional particle focusing by distorted waveforms," *Nature Physics*, vol. 12, no. 6, pp. 573–577, 2016.

[22] N. H. Aljahdaly and S. A. El-Tantawy, "Simulation study on nonlinear structures in nonlinear dispersive media," *Chaos: An Interdisciplinary Journal of Nonlinear Science*, vol. 30, no. 5, p. 53117, 2020.

[23] M. Irfan, S. Ali, S. A. El-Tantawy, and S. M. E. Ismaeel, "Three dimensional ion-acoustic rogons in quantized anisotropic magnetoplasmas with trapped/untrapped electrons," *Chaos: An Interdisciplinary Journal of Nonlinear Science*, vol. 29, no. 10, pp. 103133–103211, 2019.

[24] S. A. Almutlak, S. A. El-Tantawy, S. A. Shan, and S. M. E. Ismaeel, "Multidimensional freak waves in electron depleted dusty magnetoplasmas having superthermal ion with two temperatures," *The European Physical Journal Plus*, vol. 134, no. 10, pp. 513–515, 2019.

[25] S. A. Almutalk, S. A. El-Tantawy, E. I. El-Awady, and S. K. El-Labany, "On the numerical solution of nonplanar dust-acoustic super rogue waves in a strongly coupled dusty plasma," *Physics Letters A*, vol. 383, no. 16, pp. 1937–1941, 2019.

[26] H. Bailung, S. K. Sharma, and Y. Nakamura, "Observation of Peregrine solitons in a multicomponent plasma with negative

ions," *Physical Review Letters*, vol. 107, no. 25, pp. 255005–255014, 2011.
[27] S. K. Sharma and H. Bailung, "Observation of hole peregrine soliton in a multicomponent plasma with critical density of negative ions," *Journal of Geophysical Research: Space Physics*, vol. 118, no. 2, pp. 919–924, 2013.
[28] P. Pathak, S. K. Sharma, Y. Nakamura, and H. Bailung, "Observation of second order ion acoustic Peregrine breather in multicomponent plasma with negative ions," *Physics of Plasmas*, vol. 23, no. 2, p. 22107, 2016.
[29] D. R. Solli, C. Ropers, P. Koonath, and B. Jalali, "Optical rogue waves," *Nature*, vol. 450, no. 7172, pp. 1054–1058, 2007.
[30] D. R. Solli, C. Ropers, and B. Jalali, "Active control of rogue waves for stimulated supercontinuum generation," *Physical Review Letters*, vol. 101, no. 23, pp. 233902–233904, 2008.
[31] B. Kibler, J. Fatome, C. Finot et al., "The peregrine soliton in nonlinear fibre optics," *Nature Physics*, vol. 6, no. 10, pp. 790–795, 2010.
[32] Y. V. Bludov, V. V. Konotop, and N. Akhmediev, "Matter rogue waves," *Physical Review A*, vol. 80, no. 3, p. 33610, 2009.
[33] A. N. Ganshin, V. B. Efimov, G. V. Kolmakov, L. P. Mezhov-Deglin, and P. V. E. McClintock, "Observation of an inverse energy cascade in developed acoustic turbulence in superfluid helium," *Physical Review Letters*, vol. 101, no. 6, pp. 65303-65304, 2008.
[34] M. Shats, H. Punzmann, and H. Xia, "Capillary rogue waves," *Physical Review Letters*, vol. 104, no. 10, pp. 104503-104504, 2010.
[35] R. Höhmann, U. Kuhl, H.-J. Stöckmann, L. Kaplan, and E. J. Heller, "Freak waves in the linear regime: a microwave study," *Physical Review Letters*, vol. 104, no. 9, pp. 93901–93904, 2010.
[36] S. Vergeles and S. K. Turitsyn, "Optical rogue waves in telecommunication data streams," *Physical Review A*, vol. 83, no. 6, p. 61801, 2011.
[37] L. Stenflo and M. Marklund, "Rogue waves in the atmosphere," *Journal of Plasma Physics*, vol. 76, no. 3-4, pp. 293–295, 2010.
[38] G. Fibich, "Self-focusing in the damped nonlinear Schrödinger equation," *SIAM Journal on Applied Mathematics*, vol. 61, no. 5, pp. 1680–1705, 2001.
[39] J.-K. Xue, "Modulation of dust acoustic waves with non-adiabatic dust charge fluctuations," *Physics Letters A*, vol. 320, no. 2-3, pp. 226–233, 2003.
[40] M. Onorato and D. Proment, "Approximate rogue wave solutions of the forced and damped nonlinear Schrödinger equation for water waves," *Physics Letters A*, vol. 376, no. 45, pp. 3057–3059, 2012.
[41] M. R. Amin, "Modulation of a quantum positron acoustic wave," *Astrophysics and Space Science*, vol. 359, no. 1, pp. 2–9, 2015.
[42] M. R. Amin, "Modulation of a compressional electromagnetic wave in a magnetized electron-positron quantum plasma," *Physical Review E*, vol. 92, no. 3, pp. 33106–33117, 2015.
[43] S. Guo and L. Mei, "Modulation instability and dissipative rogue waves in ion-beam plasma: roles of ionization, recombination, and electron attachment," *Physics of Plasmas*, vol. 21, no. 11, pp. 112303–112311, 2014.
[44] S. Guo, L. Mei, Y. He, and Y. Li, "Modulation instability and ion-acoustic rogue waves in a strongly coupled collisional plasma with nonthermal nonextensive electrons," *Plasma Physics and Controlled Fusion*, vol. 58, no. 2, pp. 025014–025023, 2016.
[45] S. A. El-Tantawy, "Ion-acoustic waves in ultracold neutral plasmas: modulational instability and dissipative rogue waves," *Physics Letters A*, vol. 381, no. 8, pp. 787–791, 2017.
[46] S. A. El-Tantawy, A. H. Salas, M. M. A. Hammad, S. M. E. Ismaeel, D. M. Moustafa, and E. I. El-Awady, "Impact of dust kinematic viscosity on the breathers and rogue waves in a complex plasma having kappa distributed particles," *Waves in Random and Complex Media*, pp. 1–22, 2019.
[47] G. Fotopoulos, N. I. Karachalios, V. Koukouloyannis, and K. Vetas, "The linearly damped nonlinear Schrödinger equation with localized driving: spatiotemporal decay estimates and the emergence of extreme wave events," *Zeitschrift für angewandte Mathematik und Physik*, vol. 71, no. 1, pp. 3–23, 2020.
[48] A. Barkan, R. L. Merlino, and N. D'Angelo, "Laboratory observation of the dust-acoustic wave mode," *Physics of Plasmas*, vol. 2, no. 10, pp. 3563–3565, 1995.
[49] M. W. Morooka, J.-E. Wahlund, A. I. Eriksson et al., "Dusty plasma in the vicinity of Enceladus," *Journal of Geophysical Research: Space Physics*, vol. 116, no. A12, 2011.
[50] C. A. Mendoza-Briceño, S. M. Russel, and A. A. Mamun, "Large amplitude electrostatic solitary structures in a hot non-thermal dusty plasma," *Planetary and Space Science*, vol. 48, no. 6, pp. 599–608, 2000.
[51] P. Sethi, N. Kaur, K. Singh, and N. S. Saini, "Rogue waves in dusty plasma with two temperature superthermal," *AIP Conference Proceedings*, vol. 1925, no. 1, pp. 020013–020017, 2018.
[52] Y. Ghai and N. S. Sain, "Shock waves in dusty plasma with two temperature superthermal ions," *Astrophysics and Space Science*, vol. 362, no. 3, pp. 58–67, 2017.
[53] J.-K. Xue, "Propagation of nonplanar dust-acoustic envelope solitary waves in a two-ion-temperature dusty plasma," *Physics of Plasmas*, vol. 11, no. 5, pp. 1860–1865, 2004.
[54] M. Onorato, S. Residori, U. Bortolozzo, A. Montina, and F. T. Arecchi, "Rogue waves and their generating mechanisms in different physical contexts," *Physics Reports*, vol. 528, no. 2, pp. 47–89, 2013.
[55] M. S. Ruderman, "Freak waves in laboratory and space plasmas," *The European Physical Journal Special Topics*, vol. 185, no. 1, pp. 57–66, 2010.
[56] M. S. Ruderman, T. Talipova, and E. Pelinovsky, "Dynamics of modulationally unstable ion-acoustic wavepackets in plasmas with negative ions," *Journal of Plasma Physics*, vol. 74, no. 5, pp. 639–656, 2008.
[57] I. Kourakis and P. K. Shukla, "Ion-acoustic waves in a two-electron-temperature plasma: oblique modulation and envelope excitations," *Journal of Physics A: Mathematical and General*, vol. 36, no. 47, pp. 11901–11913, 2003.
[58] N. S. Saini and I. Kourakis, "Dust-acoustic wave modulation in the presence of superthermal ions," *Physics of Plasmas*, vol. 15, no. 12, pp. 123701–123711, 2008.
[59] J.-K. Xue, "Modulational instability of dust ion acoustic waves in a collisional dusty plasma," *Communications in Theoretical Physics*, vol. 40, no. 6, pp. 717–720, 2003.
[60] B. Kibler, J. Fatome, C. Finot et al., "Observation of Kuznetsov-Ma soliton dynamics in optical fibre," *Scientific Reports*, vol. 2, no. 1, p. 463, 2012.
[61] S. A. El-Tantawy and A. H. Salas, *A Comparison between the Semi-analytical Solution and Finite Difference Schemes for Modeling Dissipative Rogue Waves and Breathers in a Complex Plasma*, Frontires in Physics, Lausanne, Switzerland, 2020.
[62] S. A. El-Tantawy, A. T. Elgendy, and S. Ismail, "Cylindrical freak waves in a non-Maxwellian dusty bulk-sheath plasma:

an approximate solution for the cylindrical nonlinear Schrödinger equation," *Physics Letters A*, vol. 381, no. 40, pp. 3465–3471, 2017.

[63] S. A. El-Tantawy and T. Aboelenen, "Simulation study of planar and nonplanar super rogue waves in an electronegative plasma: local discontinuous Galerkin method," *Physics of Plasmas*, vol. 24, no. 5, Article ID 52118, 2017.

[64] S. A. El-Tantawy and E. I. El-Awady, "Cylindrical and spherical Akhmediev breather and freak waves in ultracold neutral plasmas," *Physics of Plasmas*, vol. 25, no. 1, pp. 12121–12126, 2018.